International Journal for Multidisciplinary Research (IJFMR)
E-ISSN: 2582-2160 ● Website: www.ijfmr.com ● Email: editor@ijfmr.com

Adaptive Confidence-Based Deep Learning Framework for Robust Detection and Classification of Paddy Leaf Diseases Under Close-Up and Far-Field Conditions

Thet Mon Myint Aung[1], Khin Mu Mu Myint[2], Khaing Win Phyu[3], Hnin Lae Wah[4]

[1,2,3,4]Department of Mechatronic Engineering, Yangon Technological University

Abstract:
Accurate detection and classification of paddy leaf diseases under varying imaging conditions remain challenging because changes in imaging distance affect the apparent size, visibility, and localization of disease symptoms. This study proposed an adaptive confidence thresholding for robust detection and classification of healthy and five paddy leaf diseases under close-up and far-field conditions. YOLOv9-e, a single-stage detector, and ResNet-18 + R-CNN, a two-stage detector, were comparatively evaluated using fixed and adaptive confidence thresholding schemes. The experimental results revealed distinct prediction characteristics between the two detection architectures. YOLOv9-e generally produced more precise and compact predictions, whereas ResNet-18+R-CNN generated denser and more overlapping predictions. Both models achieved better detection performance for close-up images than for far-field images, reflecting the increased difficulty of detecting smaller and less distinguishable disease regions in far-field scenes. When applying adaptive confidence thresholding, YOLOv9-e improved its accuracy from 62.15% to 91.50% and ResNet-18+R-CNN enhanced the accuracy from 3.80% to 36.58%. Furthermore, applying adaptive thresholding reduced the performance gaps between close-up and far-field conditions for both deep learning models. Overall, the findings indicate that adaptive confidence thresholding can enhance the robustness of deep learning-based paddy leaf disease detection, particularly under challenging far-field conditions.

Keywords: Adaptive confidence threshold, paddy disease detection, deep-learning framework, leaf disease classification, far-field detection

1. Introduction

Today, rice (paddy) leaf disease detection and classification becomes an essential research area critical for safeguarding food security, preventing severe crop yield losses, and mitigating economic damage caused by bacterial, fungal, and viral pathogens[1], [2]. Timely diagnosis is important for supporting precision agriculture, enabling target treatments, and reducing unnecessary pesticide use. However, this research area remains challenging due to the high visual similarity among distinct diseases such as distinguishing between “Brown Leaf Spot”, “Narrow Brown Leaf Spot” and “Rice Blast”, as well as

noisy field conditions, variable lighting conditions, far-field and close-up conditions. Consequently, advanced technologies like machine learning and deep learning have become essential tools; by leveraging Convolutional Neural Networks (CNNs), transfer learning, and hybrid architectures, thereby enabling faster, more accurate, and automated disease diagnosis. Thus, several key studies have proposed evaluated diverse machine learning and deep paradigms to improve the performance by overcoming the challenges [3], [4].

In earlier studies by Narmadha et al., (2017) and Prajapati et al., (2017), machine learning models (SVM, KNN) combined with color-space transformations and feature extraction, paddy leaf diseases were applied[5],[6]. However, heavily relying on hand-crafted features that sensitive to lighting variations and background clutter make them less adaptable to variable views. Until recent years, some studies [7], [8] still applied multi-class SVM optimized SVM coupling with K-means and Level Set segmentation methods for classifying four different paddy leaf diseases. However, these classification methods are sensitive to field lighting fluctuations and/or computationally heavier. Wijayanto et al., (2024) evaluated the performance of Random Forest (RF) classifier and Neural Network (NN) for Bacterial Leaf Blight (BLB) [9]. It was found that Random Forest (RF) consistently outperformed Neural Networks (NN) across all tested scenarios.

Although some machine learning approaches are promising, studies are turning into advanced deep learning paradigms and transfer learning because plant-disease images contain complex, variable, and spatially distributed visual patterns that are difficult to represent with manually designed features, while deep learning can simultaneously localize and classify disease symptoms [10]. Some of previous studies simply fine-tuned and evaluated pretrained models while some other studies modified pre-trained CNN models to enhanced the performance.

Matin et al., (2020) fine-tuned AlexNet architecture to detect three major rice leaf diseases [11]. Babu et al.,(2022) applied ResNet (101 layers), Inception v4 (16 layers), VGGNet (16 layers), and DenseNet (121 layers) [12]. Petchiammal and Murugan (2025) reported that DenseNet121 achieved the best performance among the evaluated pretrained models [13]. Padhi et al., (2025) evaluated ResNet-18 CNN architectures for rice leaf disease classification. The authors identified Darknet53 as the most effective baseline model [14]. Mehnaz and Islam, (2025) conducted a systematic comparative evaluation across three distinct machine learning paradigms; traditional Machine Learning, Convolutional Neural Networks (ResNet50, ResNet152, Inception-V3), and Vision Transformers (MaxViT-L)[15]. From these studies, only the base line performance of pre-trained deep learning models comparatively discovered.

Related to modified CNN models, Ramesh and Vydeki (2020) used Optimized Deep Neural Network Jaya Optimization Algorithm to automatically optimize and select the best node weights [16]. Singh et al., (2026) investigated the performance of modified DenseNet architectures by integrating SE block [17]. Tasci (2026) also integrated MobileNet with SE block [18]. Altabaji et al., (2024) evaluated modified LeafNet architecture against the baseline LeafNet, as well as pre-trained Xception and MobileNetV2 architectures [19]. Mahadevan et al., (2024) proposed improved threshold neural network (ITNN) for detection and analysis of rice diseases [20]. These studies showed that modifying existing CNN model can somewhat enhance the performance.

Some existing studies attempted for achieving light-weight models to be practically applicable on edge devices. Joseph et al., (2024) proposed lightweight custom CNN for Maize, Rice, Wheat plant diseases classification [21]. Bijoy et al. (2024) proposed lightweight custom dCNN across environmental scenarios such as natural backgrounds, down-sampling/up-sampling, different camera rotation, zoomed-out distances, different light intensity [22].

In recent years, hybrid-models have become attractive for balancing light-weight and performance. Rodrigo et al. (2024) proposed a hybrid architecture which combines local feature extraction from CNNs with global context learning from Vision Transformers (ViTs)MobileViTV2. The model significantly outperforms traditional CNNs in accuracy [23].
Mahmud et al. (2025) applied ResNet50, ResNet101, VGG16, MobileNetV2 by integrating XAI techniques for classifying paddy leaf conditions; Healthy, Tungro, and Brown Spot. The authors concluded that integration of filtering edge detection with deep learning architectures delivered highly reliable automated disease detection[24]. Although the performances of these innovative methods were favorable, the performance evaluation was only based on classification excluding localization.

In these days, YOLO model variants have received considerable attention in recent plant disease detection research. Jain et al., (2022) evaluated YOLOv3 tiny and YOLOv4 tiny models for identifying paddy diseases “Brown spot”, “Leaf blast” and “Hispa” where YOLOv4 tiny achieved a higher performance [25]. Abid et al. (2024) attempted to evaluate the performance of YOLOv8 for detection of healthy and diseased states across Rice, Corn, Wheat, Potato, and Tomato [26]. The authors used confidence threshold of 0.654 and observed that the performance was lowest for rice diseases, specifically rice brown spot. Abid et al. (2024) worked with YOLOv8 for “Brown Spot”, “Hispa”, “Blast”, “Blight” and achieved average accuracy of 94% [26]. A comparative analysis on the performance of YOLOv8 and YOLOv9 was conducted in [27] for detection of plant diseases in hydroponics system. In terms of accuracy YOLOv9 showed a better performance while YOLOv8 was favorable for processing time. Sudharshan et al., (2025) evaluated YOLOv9 (especially YOLOv9s) against YOLOv8, Faster R-CNN, SSD, and ResNet-50 + FPN for paddy leaf disease classification[28]. The results showed the YOLOv9 have slightly better performance with an optimum confidence threshold was 0.57. Then, Zope et al., (2024) fine-tuned YOLOv9 architecture fine-tuned for detection and classification of pigeon pea leaf diseases [29]. The authors observed YOLOv9 gave low performance for “Black Spot” and even failed to detect “Leaf Mold” diseases. It could be because of setting a high and constant confidence threshold.

When synthesizing the existing studies in the literature, we observed multiple critical research gaps as follows; (1) previous research studies did not consider adaptive confidence thresholding scheme since YOLO many not effectively work for different leaf diseases with constant confidence thresholding, (2) comparative evaluation of single-stage detection model (YOLOv9) and light-weight two-stage detection model (ResNet-18 + R-CNN), (3) evaluation of deep learning model for both close-up view and far-field view of paddy leaf diseases.
The objectives of this study are to perform (1) a comparative performance analysis of YOLOv9 (single-stage model) and ResNet-18 + R-CNN (two-stage model) using fixed and adaptive confidence

thresholding schemes and (2) evaluation of selected deep learning models for close-up view and far-field view of six different paddy leaf diseases.

2. Methodology

2.1 YOLOv9 and ResNet-18 + R-CNN Models

YOLOv9 was introduced by Wang et al., (2024), represents a major evolution in real-time object detection by addressing a fundamental issue in deep network training: information loss as input data passes through deep layers [30] . YOLOv9 introduces Programmable Gradient Information (PGI) to combat the degradation of gradient information necessary for target object features to be properly learned. Alongside PGI, YOLOv9 introduces GELAN, a novel lightweight network architecture designed to optimize parameter usage, computational efficiency simultaneously. Combining PGI and GELAN variants ranging from tiny structures (YOLOv9-T, YOLOv9-S) up to extensive architectures (YOLOv9-E) achieve significantly higher parameter efficiency and detection accuracy. A more detailed information of YOLOv9 and discussion can be seen in [30] . In this study, only YOLOv9-e was selected as single-stage deep learning model.

To conduct a comparative evaluation with YOLO variants (single-stage detection model), a two-stage detection model was constructed by combining ResNet-18 and R-CNN. The integration of a ResNet-18 as backbone creates a lightweight detection pipeline that balances memory footprint with robust feature extraction. ResNet-18 serves as the initial convolutional feature extractor. Faster R-CNN feeds the backbone's feature map into an RPN. The RPN uses sliding windows over anchor box configurations to evaluate objectness scores and output high-confidence candidate region proposals. The proposed regions and the shared feature maps are processed through an RoI pooling. Then, fully connected layers then execute final class predictions and bounding box regressions [31], [32].

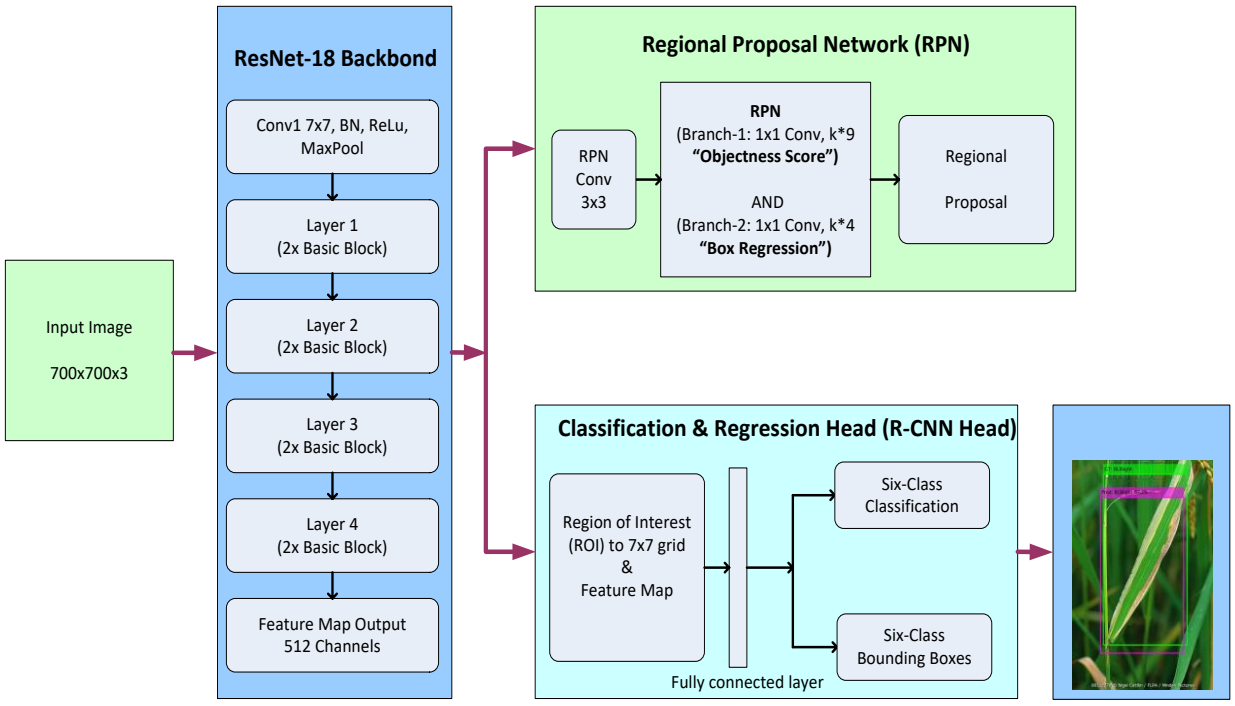


Figure.1. ResNet-18+R-CNN Architecture

2.2 Fixed and Adaptive Confidence Thresholds

Figure 2 and Figure 3 shows the detection pipelines of YOLOv9-e (single-stage detection model) and ResNet-18+RCNN (two-stage detection model).

In YOLOv9-e (single-stage) detection pipeline, the detection head bifurcates into two output streams: bounding box coordinate parameters of detected objects and probabilistic scores associated with each object class. To refine the detection quality, the class confidence scores pass through a fixed or adaptive confidence threshold. With fixed threshold, a rigid confidence value was applied for filtering detected object. If it is adaptive threshold, it dynamically adjusts the cutoff limits based on score distributions. The thresholded confidence scores, alongside the corresponding bounding boxes, are then processed by Non-Maximum Suppression (NMS) to eliminate redundant overlapping detections. Finally, the processed outputs generate the final prediction, which are evaluated against ground truth annotations to measure model performance.

In ResNet-18+R-CNN (two-stage) detection framework, the feature extraction is handled by a ResNet-18 backbone, followed by a Regional Proposal Network (RPN) that generates candidate objectness scores and bounding box regressions.

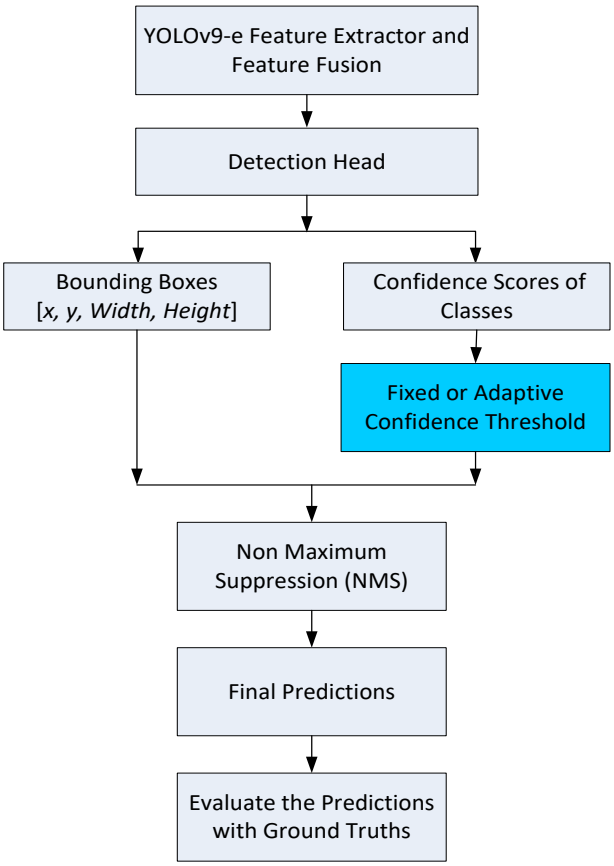


Figure.2. Detection pipeline of YOLOv9

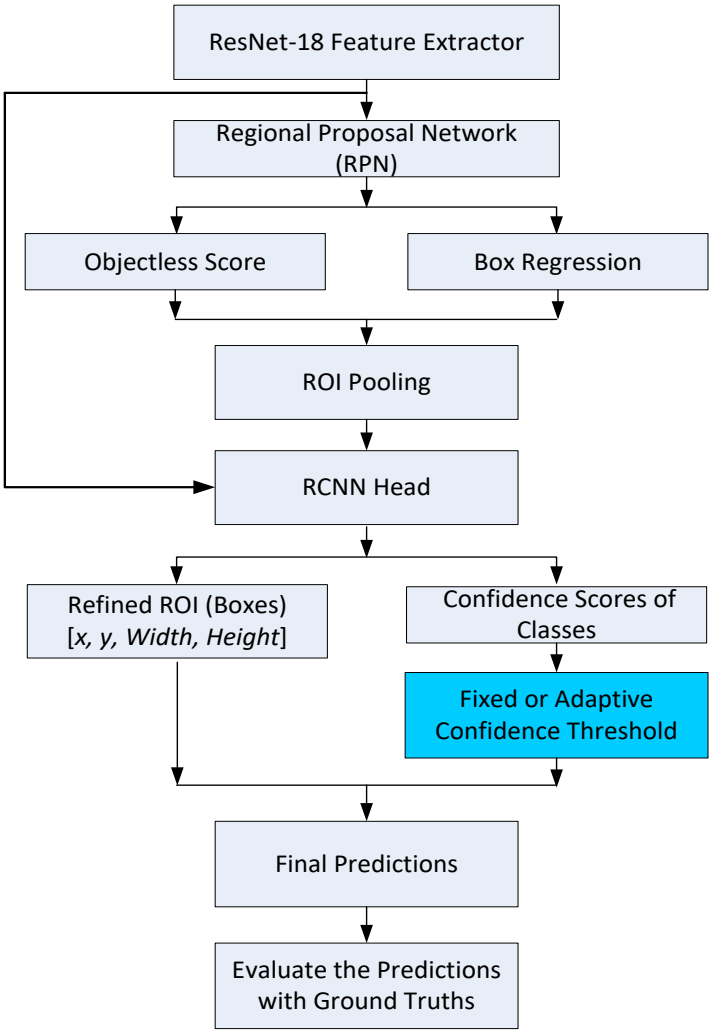


Figure.3. Detection pipeline of ResNet-18+R-CNN

After ROI pooling and feature refinement through the R-CNN head, the network branches into two parallel paths: one outputting refined bounding box coordinates and the other yielding class-specific confidence scores.

To optimize detection performance under varying object scales or scene complexities, the class confidence scores pass through a fixed or adaptive confidence threshold. This filtered set of confidence scores is then combined with the refined ROIs to generate the final predictions, which are subsequently evaluated against ground truth annotations.

For the case of paddy leaf diseases, assigning fixed thresholding can cause even fail in detection as in the study of Zope et al., (2024) [29]. Thus, in this work adaptive confidence thresholding is applied and evaluated for paddy leaf diseases which have different textures. To apply the adaptive confidence thresholds, candidate classes are first collected with very low confidence, 0.02, then among many detections, the maximum confidence value was set as the adaptive confidence threshold. The prediction with the highest confidence value is retained as the final predicted result.

2.3 Paddy Leaf Diseases, Close-Up View and Far-Field View

Being susceptible to various fungal and bacterial diseases that can reduce photosynthetic activity, paddy leaves can suffer from different diseases[33]. In this study, as shown in Figure 4, six paddy leaf classes

are considered: Bacterial Leaf Blight (BLBlight), Bacterial Leaf Streak (BLStreak), Brown Leaf Spot (BLSpot), Narrow Brown Leaf Spot (NBLSpot), Rice Blast (RBlast), and Healthy. These classes were selected because their symptoms can exhibit similar and they are still providing a challenging and representative problem for image-based disease detection and classification.

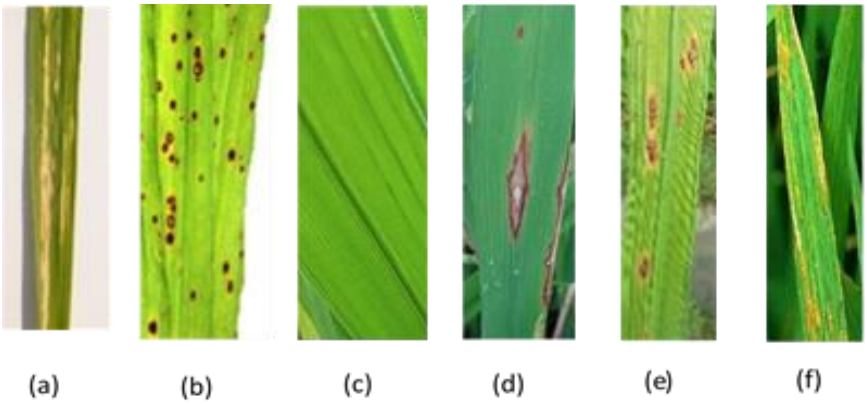


Figure.4. Healthy and five different paddy leaf diseases
(a) Bacterial Leaf Blight (b) Brown Leaf Spot (c) Healthy
(d) Rice Blast (e) Narrow Brown Leaf Spot (f) Bacterial Leaf Streak

In this study, both close-up and far-field views of paddy leaf diseases are considered. In a close-up view, disease symptoms occupy a relatively large portion of the image, allowing fine visual characteristics such as lesion shape, color, texture, and boundaries to be captured with greater detail. This condition is generally more informative for distinguishing visually similar disease classes.

In contrast, as shown in Figure 5, a far-field view represents a more challenging and practical observation condition in which a larger portion of the leaf canopy is captured from a greater distance. Disease symptoms occupy fewer pixels and may therefore become small.

Furthermore, variations in illumination, leaf orientation, overlapping leaves, and environmental background can increase detection difficulty. Therefore, the performance of two different deep learning models were tested for both close-up view and far-field view.

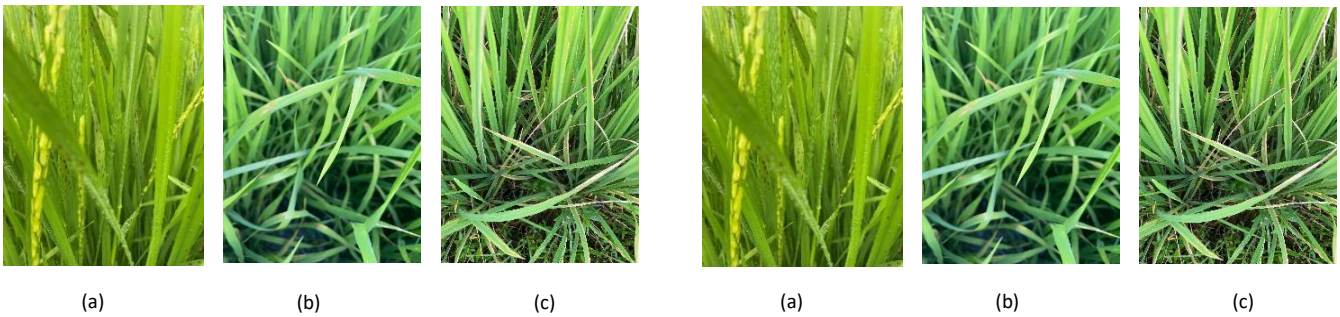


Figure.5. Far-field view of paddy leaf diseases (a)
(b) Brown Leaf Spot (b) Bacterial Leaf Blight
(c) Bacterial Leaf Streak

2.4 Datasets Used in Training, Validation and Testing

In this study, both available dataset and our own dataset were used to evaluate the performance of selected deep learning frameworks. The dataset contains images representing visual appearances of healthy and five different diseases namely Bacterial Leaf Blight (BLBlight), Bacterial Leaf Streak (BLStreak), Brown Leaf Spot (BLSpot), Healthy, Narrow Brown Leaf Spot (NBLSpot), and Rice Blast (RBlast). The close-up view images are taken from the dataset available in the literature [33]., Then, the dataset of far-field view images is our own dataset captured by using a phone camera with a maximum resolution of 50 MP. The leaf disease images were taken from Daydaye Township, Ayeyarwady Division and Thanlyin Township, Yangon Division of Myanmar.

The total number of training images is 2058 which include 343 for each class. A total of 660 images were used for validation and 660 images were used for testing. Here, only close-up views of paddy leaf diseases were trained and both close-up view and far-field view images were used for testing. The ground truth annotations were implemented in rectangle bounding boxes as shown in Figure 6.



Figure.6. Samples of annotated images

The train-validation-test data split is shown in Table 1. In training process, a balanced class distribution was maintained, with a similar number of images allocated to each of the healthy and five disease classes.

In training both deep learning frameworks, the essential training parameters such as number of training epochs, image resolution, optimizer, augmentation, hardware, annotation format are kept the same for fair comparison.

Table 1 Train-validation-test data split

View	Train Images	Validation Images	Test Images
Close-up View	2058	450	450
Far-field View	-	210	210

2.5 Performance Evaluation Metrics

The performances of the developed deep learning models were evaluated using several commonly used classification and object-detection performance metrics, including accuracy, precision, recall, F1-score, and Intersection over Union (IoU). These metrics were selected to provide a comprehensive assessment on the performance of YOLOv9 (single-stage detection) and ResNet-18+R-CNN (two-stage detection) to localize (detect) disease regions and to correctly identify paddy leaf diseases. The performance evaluation metrics can be mathematically expressed as follows.

$$Accuracy=TP+TN/(TP+FP+FN+TN) \quad (1)$$

$$P= TP/(TP+FP) \quad (2)$$

$$R= TP/(TP+FN) \quad (3)$$

$$F1=(2*P*R)/(P+R) \quad (4)$$

$$mAP=1/N \sum_(i=1)^N AP \quad (5)$$

where, P is precision, R is recall, F1 is F1 score, mAP is mean Average Precision, TP is True Positive, FP False Positive, FN is False Negative and TN is True Negative.

3. Results and Discussions

3.1 Qualitative Observations

Figure 7 presents a qualitative comparison of the detection results obtained using YOLOv9-e model. The results for close-up views are arranged in Figure 7 (a) and the results for far-field view are in Figure 7 (b). The results in upper row were achieved by using YOLOv9-e and the results in lower row were achieved by using ResNet-18+R-CNN. The results are free detections without specific ground truth annotations. For fair comparison, both models were set with the same confidence threshold and Non-Maximum Suppression (NMS) threshold.

As illustrated in the upper row of Figure 7 (a), YOLOv9-e produces a small number of bounding boxes compared to ResNet-18+R-CNN model for every disease type. For example, YOLOv9-e model successfully localizes regions associated with Bacterial Leaf Blight, Bacterial Leaf Streak, and Narrow Brown Leaf symptoms while avoiding a large number of additional predictions. This indicates that YOLOv9-e can effectively exploit the spatial and visual features of disease symptoms in close-up images.

In contrast, the ResNet18+RCNN model shown in the lower row Figure 7 (a), generates a substantially larger number of predictions. Several predicted bounding boxes have relatively higher confidence values compared to predictions of YOLOv9-e. Although some of these predictions correctly overlap the disease regions, additional detections are observed around neighboring leaf areas. This behavior indicates that the two-stage ResNet-18+R-CNN detector can identify potential disease-related regions but may produce more candidate detections that require higher confidence filtering and non-maximum suppression.

The results also demonstrate the importance of confidence-threshold selection for single stage and two-stage detection schemes. When a relatively low confidence threshold is applied, ResNet-18+R-CNN retains a larger number of candidate detections, including several low-confidence predictions. Increasing the confidence threshold can reduce these false or unnecessary detections. Overall, the close-up examples demonstrate that both YOLOv9 and ResNet-18+R-CNN possess the capability to localize visible paddy leaf disease symptoms, but they exhibit different prediction behaviors.

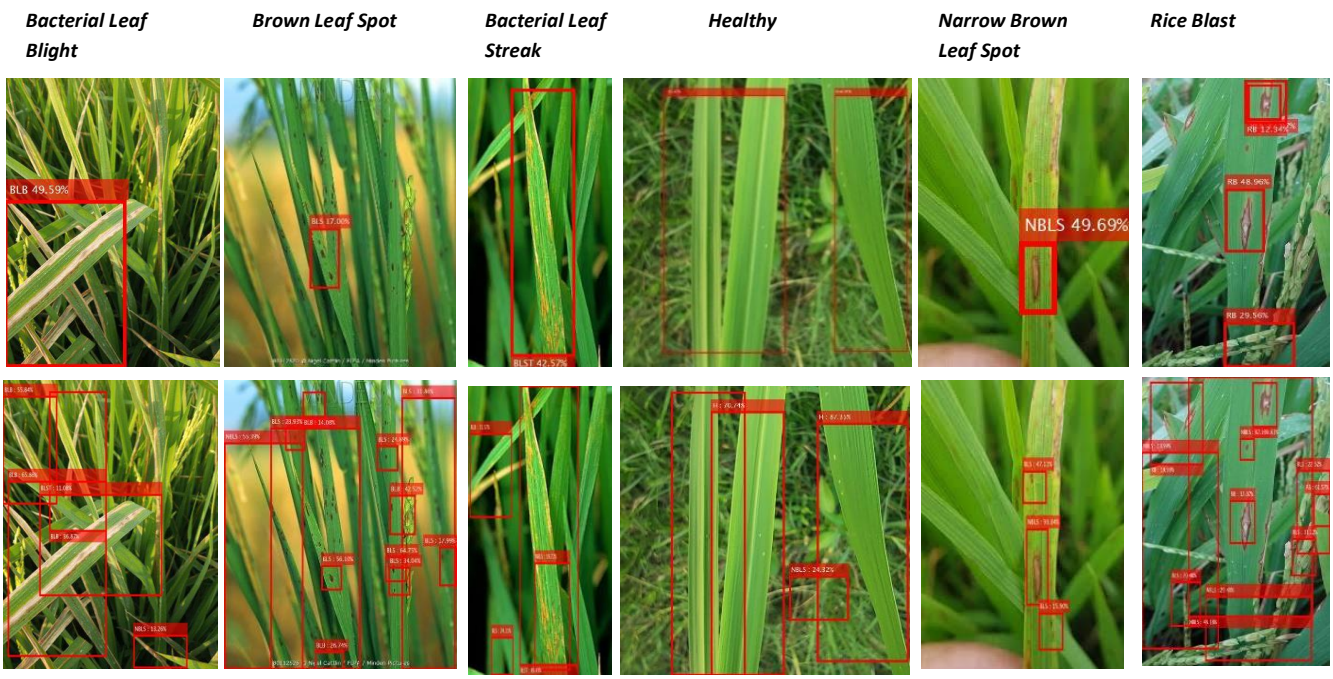
The comparative detection performance of YOLOv9-e and ResNet-18+R-CNN for detecting paddy leaf diseases in far-field views (shown in Figure 7 (b)) also reveals YOLOv9-e demonstrates cleaner and more precise bounding box localization across categories such as Bacterial Leaf Blight, Brown Leaf Spot, and Rice Blast. The model maintains sparse and targeted predictions, effectively isolating infected regions without generating excessive overlapping boxes.

In contrast, in lower row of Figure 7 (b), the ResNet-18+R-CNN architecture exhibits significantly denser and heavily overlapping bounding boxes, particularly in paddy leaf diseases like Brown Leaf Spot and Rice Blast. This behavior indicates increased prediction redundancy for the evaluated ResNet-18 + R-CNN configuration in the tested agricultural images.

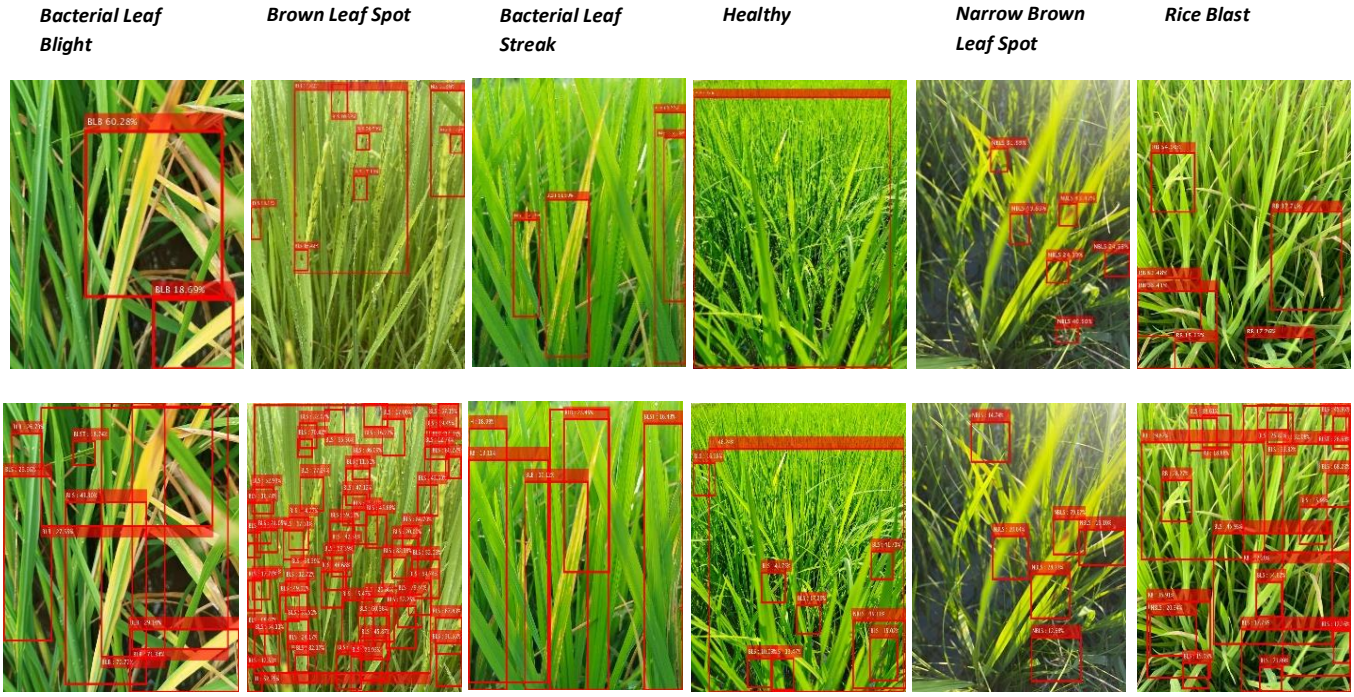
3.2 Performance of Models with Fixed Confidence Threshold

To quantitively evaluate the performance of the models, the predictions were evaluated against ground truth annotations for both close-up view and far-field view images. Figure 8 shows some sample results for predicted results and ground truth annotated. The green colour was used for ground truth annotations and magenta colour was used for predictions.

Evaluating YOLOv9-e (left) and ResNet-18+R-CNN (right) under fixed confidence thresholds highlights fundamental differences in prediction calibration, false-positive rates, and box redundancy for close-up views. YOLOv9-e demonstrates more concentrated predictions, whereas ResNet-18+R-CNN triggers multiple scattered boxes with varying class probabilities. This indicates that the two-stage framework (ResNet-18+R-CNN) is more prone to false positives or fragmented feature interpretation under complex background interference.



(a)



(b)

Figure.7. Sample results by using YOLOv9-e (Upper row) and ResNet-18+R-CNN (Lower row)
(a) close-up views, (b) far-field views

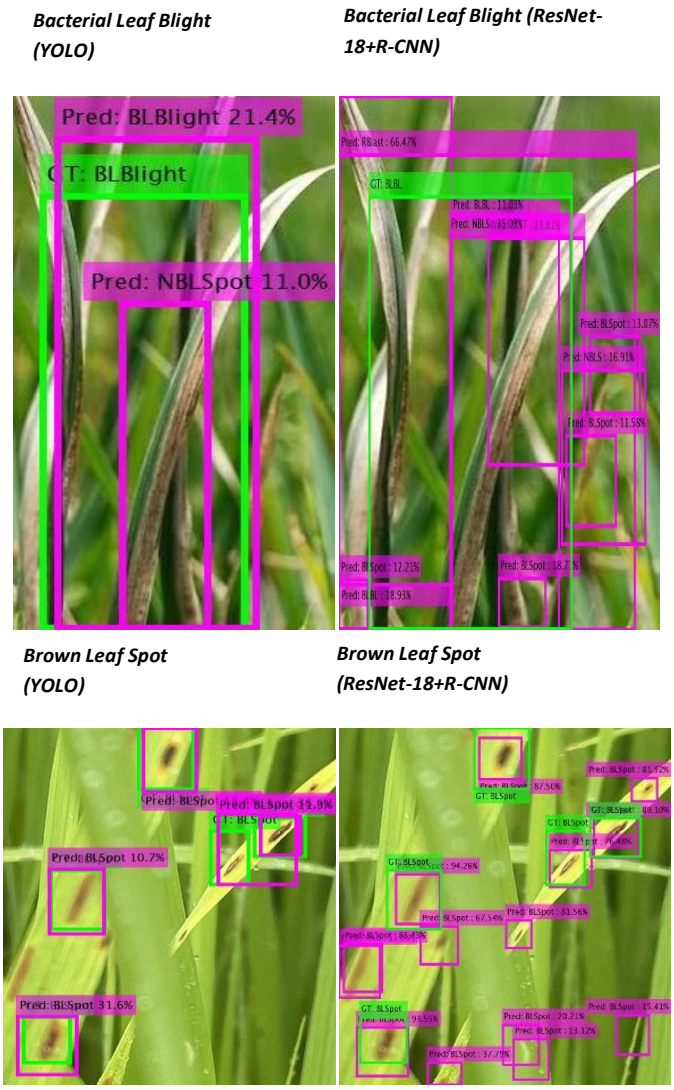


Figure.8. Sample predictions and ground truths for close-up views

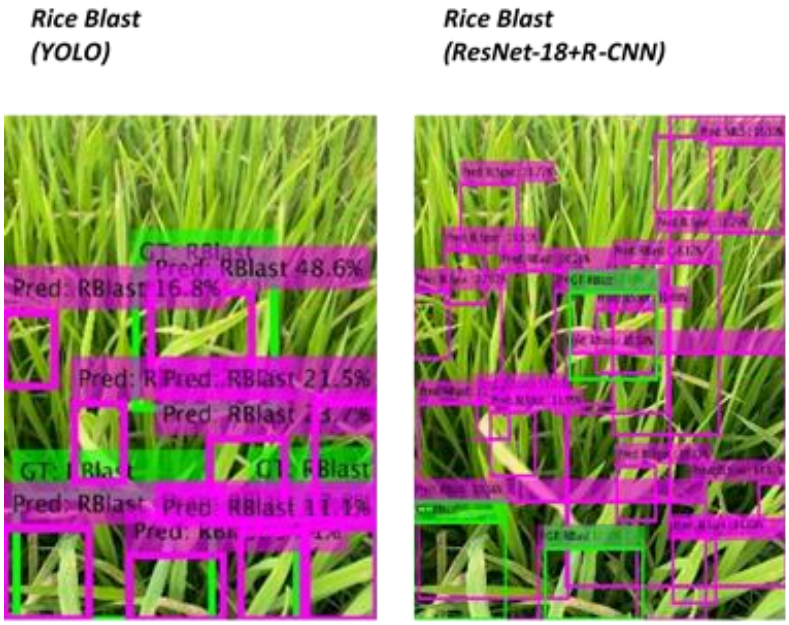
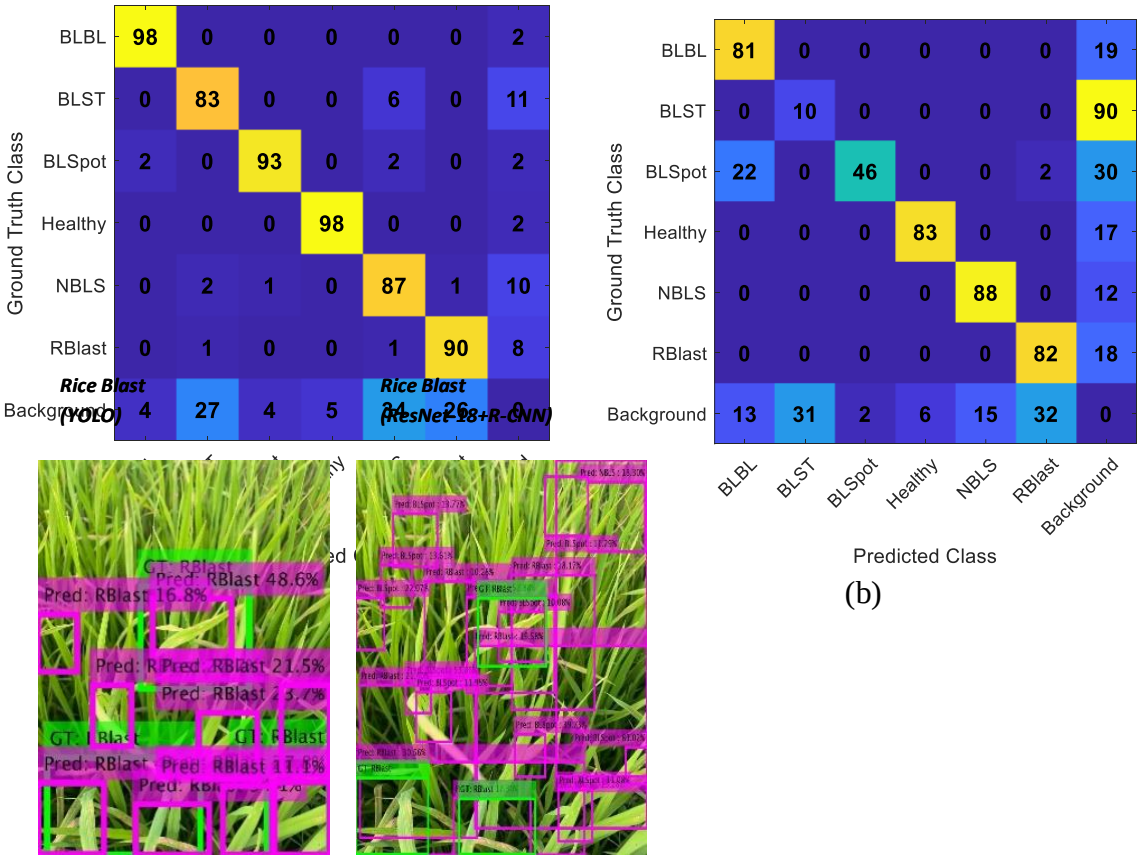
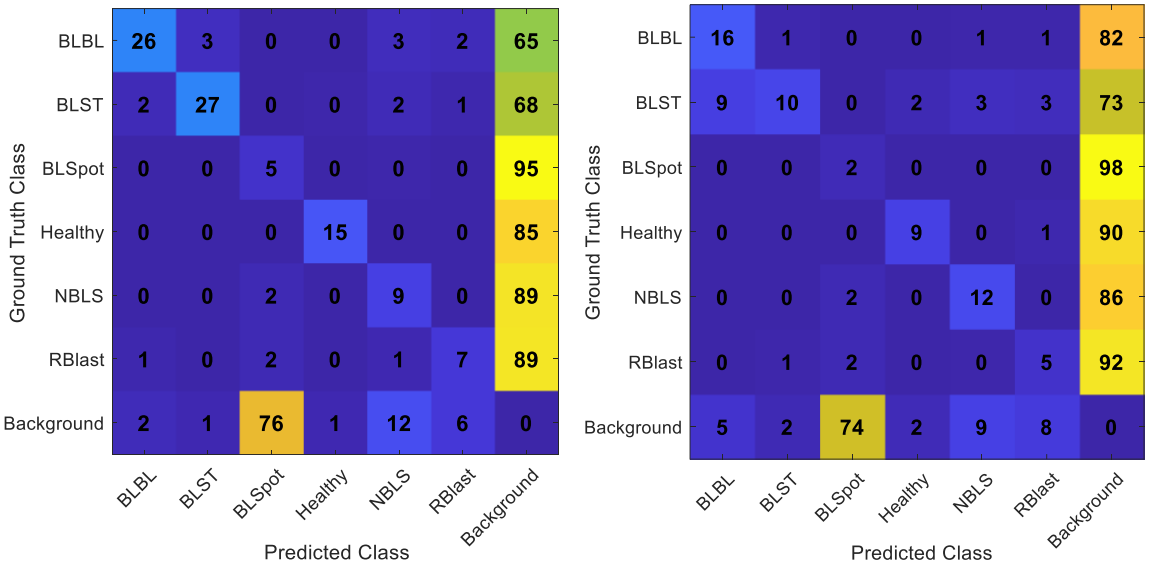


Figure.9. Sample predictions and ground truths
for far-field views

Evaluating far-field views of Rice Blast, shown in Figure 9, highlights how different architectures manage dense canopy backgrounds. Also, it can be seen that YOLO model demonstrates a more controlled distribution of prediction boxes (magenta) relative to the ground truth labels (green). Meanwhile ResNet-18+R-CNN produced an overwhelming number of overlapping bounding boxes, frequently confusing background texture with disease symptoms and introducing mixed predictions.



(b)



(c) (d)

Figure.10. Confusion matrices (a) YOLOv9-e close-up view (b) YOLOv9-e far-field view (c) ResNet-18+R-CNN close-up view (d) ResNet-18+R-CNN far-field view

Figure 10 shows the comparison of confusion matrices between two models; YOLO (upper row) and ResNet-18 + R-CNN (lower row)—across two distinct imaging conditions: close-up (left column) and far-field (right column). The YOLOv9-e results show strong, class-wise performance with a dominant diagonal (values mostly ranging from 83% to 98%) for close-up views. Misclassifications and background confusion are minimal, indicating that YOLOv9-e successfully isolates and categorizes targets when they are near. Then YOLOv9-e shows a moderate drop in accuracy under far-field conditions. The performance of Healthy remain relatively robust.

Using ResNet-18+R-CNN, a large portion of true instances is heavily misclassified into the background category even for close-up views. Both models show a slight drop of performance for far-field views.

3.3 Performance of Models with Adaptive Confidence Threshold

For evaluating the models using adaptive confidence thresholding, first all the detected results that are larger than 0.02 were collected. Then, from all detected results, the maximum confidence value was set as adaptive confidence threshold. The main idea of using adaptive confidence threshold is to remove unreliable prediction that can lead to False Positive (FP) or False Negative (FN). Thus, only one obvious and potential region from each image was annotated and used as ground truth disease region. Then, only one prediction with the highest confidence was taken to evaluate it by comparing with ground truth region and class.

The visual comparison illustrates the performance of YOLOv9-e and ResNet-18+R-CNN under different viewing conditions, contrasting a close-up view (first row) with a far-field view (second row). In the close-up views, the disease on the paddy leaf is prominent and clear. For far-field views, the disease region is mixed with a dense rice canopy.

The upper row in Figure 11 demonstrates a detection results using YOLOv9-e matching the ground truth (BLBlight) with a moderate confidence score of 49.6%. In comparison, ResNet-18+R-CNN produced

the (BLBlight) prediction with 60% confidence, but the IoU ratio is less than YOLOv9-e's prediction. For far-field view, ResNet-18+R-CNN even failed to predict.

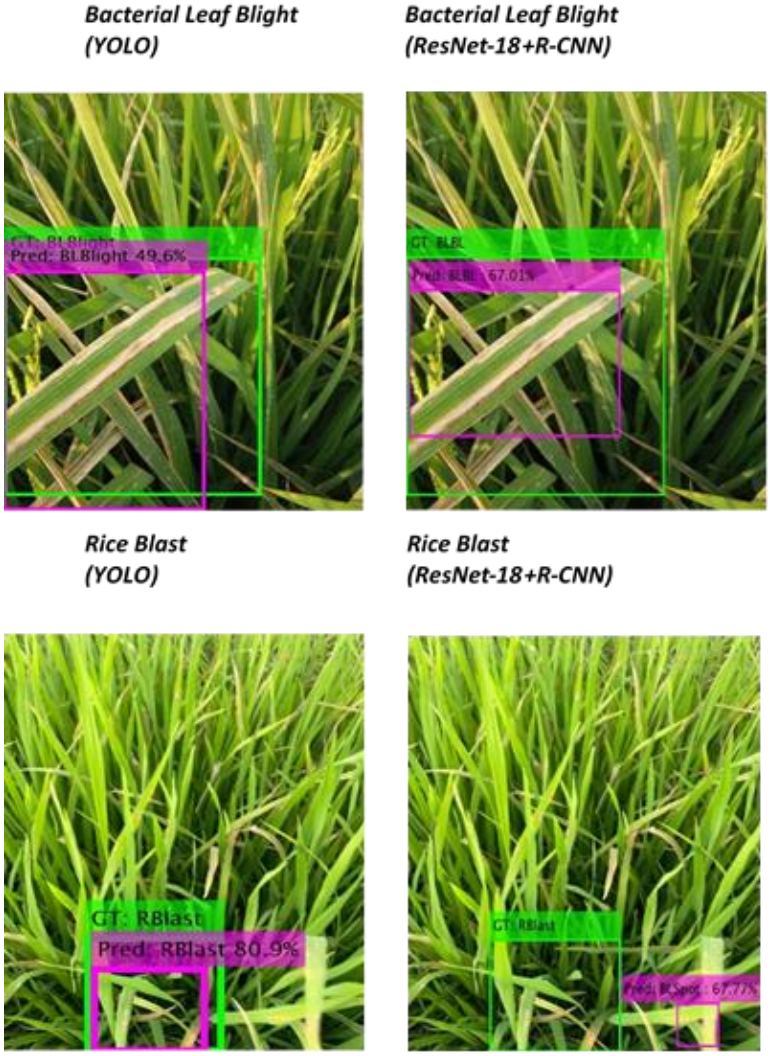


Figure.11. Sample predictions and ground truths using adaptive confidence thresholding (Upper row: close-up views, Lower row: far-field views)

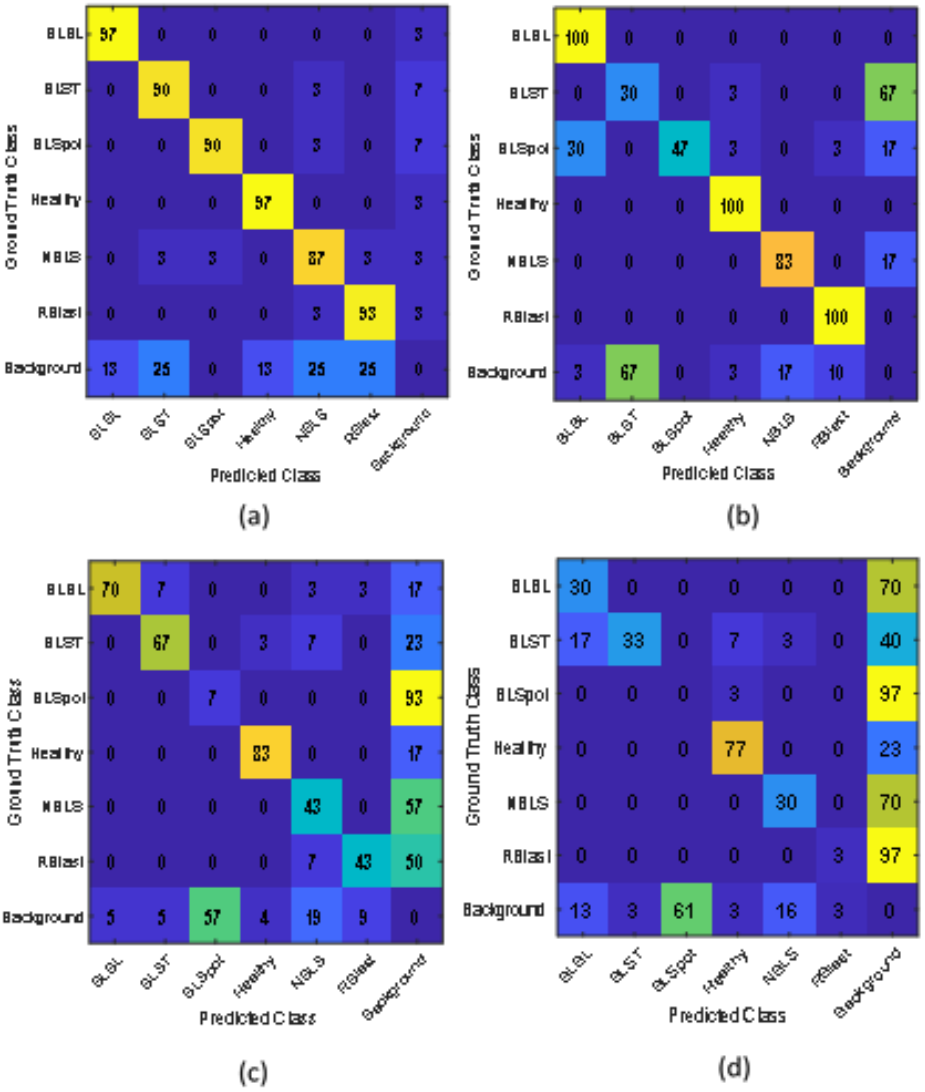


Figure.12. Confusion matrix (a) YOLOv9-e close-up
(b) YOLOv9-e far-field (c) ResNet-18+R-CNN close-up
(d) ResNet-18+R-CNN far-field

Figure 12 shows the comparison of confusion matrices achieved by using adaptive confidence thresholding in YOLOv9-e and ResNet-18+R-CNN. For the close-up condition, in Figure 12 (a), YOLOv9 exhibited strong class-wise discrimination under adaptive confidence thresholding, as indicated by the high values along the main diagonal of the confusion matrix. The displayed percentages of correct-classes rate ranged from 87% to 97% across the six disease categories. Bacterial Leaf Blight and Healthy achieved the highest values of 97%, followed by Rice Blast (93%), Bacterial Leaf Streak and Brown Leaf Spot (90%), and Narrow Brown Leaf (87%). The relatively limited off-diagonal responses suggest that the visually distinctive disease symptoms in close-up images can be effectively localized and classified by YOLOv9-e. Under the far-field condition, in Figure 12 (b), YOLOv9-e maintained high correct-class responses for several categories, including Bacterial Leaf Blight, Healthy, and Rice Blast. However, greater class confusion was observed for Bacterial Leaf Streak and Brown Leaf Spot, together with increased association with the Background class.

The results obtained using ResNet-18+R-CNN, Figure 12 (c), show greater variability among the disease categories. The highest displayed correct-class response was obtained for Healthy (83%), followed by Bacterial Leaf Blight (70%) and Bacterial Leaf Streak (67%). For far field view, Figure 12 (d), results of ResNet-18+RCNN demonstrate the greatest degradation in class-wise detection performance. This behavior suggests that the small spatial extent of disease symptoms in far-field images presents a substantial challenge for the ResNet-18+R-CNN architecture.

3.4 Overall Performance Comparison

For giving a comprehensive understanding on the performances of two different deep learning frameworks, overall performance comparison was made. Table 2 shows the performance matrices are average accuracy, recall, precision and F1 score at fixed and adaptive confidence thresholding and close-up view and far-field views.

Table 2 Overall performance comparison under fixed and adaptive confidence thresholds

Deep Learning Framework	View	Accuracy (%)	Precision (%)	Recall (%)	F1 score (%)	mAP@0.5
Using Fixed Confidence Thresholding						
YOLOv9-e	**Close- Up**	62.15	65.64	92.12	76.66	0.69
	Far-Field	30.08	42.35	60.15	49.71	0.46
ResNet-18+R-CNN	**Close- Up**	3.80	16.65	12.50	14.28	0.19
	Far-Field	2.89	13.13	7.79	9.78	0.15
Using Adaptive Confidence Thresholding						
YOLOv9-e	**Close- Up**	91.50	95.56	95.56	95.56	0.92
	Far-Field	71.43	83.33	83.33	83.33	0.78
ResNet-18+R-CNN	**Close- Up**	36.58	50.40	44.76	47.41	0.59
	Far-Field	17.39	33.45	24.76	22.88	0.39

The empirical results demonstrate distinct performance paradigms between modern single-stage anchor-free architectures and traditional region-proposal frameworks.

Under fixed confidence thresholding, YOLOv9-e exhibits superior baseline performance, particularly in close-up scenarios where it achieves an accuracy of 62.15%, a high recall of 92.12%, and an F1 score of 76.66. Conversely, the ResNet-18+R-CNN model struggles significantly in this configuration, yielding a close-up accuracy of only 3.80% and an F1 score of 14.28%. When transitioning to far-field views, both frameworks experience performance degradation due to scale variations and reduced feature resolution,

though YOLOv9-e retains a markedly higher accuracy of 30.08% compared to ResNet-18+R-CNN's 2.89%.

Compared with fixed confidence thresholding, adaptive confidence thresholding substantially improved the measured performance across the evaluated configurations. For YOLOv9-e, close-up accuracy surges to 91.50%, accompanied by identical precision, recall, and F1 scores of 95.56%. Similarly, the far-field accuracy for YOLOv9-e escalates to 71.43%, with precision, recall, and F1 metrics leveling at 83.33%. While ResNet-18+R-CNN also benefits from adaptive thresholding—raising its close-up accuracy to 36.58% and far-field accuracy to 17.39%—its overall metrics remain substantially lower than those of the YOLOv9-e architecture.

The empirical findings underscore the critical role of thresholding strategies in object detection robustness. Adaptive thresholding mitigates the limitations associated with rigid confidence, allowing models to dynamically adjust to varying environmental contexts and object scales. Furthermore, the mAP@0.5 values show that the YOLOv9 model performs better for the close-up images than for the far-field images and also the same situation was observed with ResNet-18+RCNN.

4. Conclusion

This study presented a comparative evaluation of YOLOv9-e, representing a single-stage object detection architecture, and ResNet-18+R-CNN, representing a two-stage detection architecture, for the detection and classification of six paddy leaf diseases under close-up and far-field imaging conditions. In addition, the study investigated the effectiveness of adaptive confidence thresholding schemes on the detection performance of both models compared to fixed confidence thresholding.

The experimental results demonstrated that YOLOv9-e generally produced more precise and compact detections, with predictions more closely localized to the annotated disease regions. In contrast, ResNet-18+ R-CNN tended to generate denser predictions, including overlapping bounding boxes and detections extending into non-object or background regions. These differences indicate that the architectural characteristics of single-stage and two-stage detectors can substantially influence the localization behavior of paddy leaf disease detection.

For both models, the close-up view generally resulted in better detection performance than the far-field view. Nevertheless, the application of adaptive confidence thresholding improved the overall robustness of both detection models compared with a fixed confidence threshold. In particular, adaptive thresholding helped maintain detection performance under far-field conditions, resulting in less performance degradation compared with the corresponding fixed-threshold approach.

Among the evaluated configurations, YOLOv9-e with adaptive confidence thresholding achieved the highest measured performance across the tested close-up and far-field conditions. Adaptive confidence thresholding method indicates its potential for paddy leaf disease detection under varying image acquisition conditions. The observed performance difference may be related to architectural and capacity differences between the two evaluated models; however, this relationship was not directly investigated in this study.

Despite these findings, the present study has some limitations. The investigation was conducted using a limited number of detection architectures and a particular adaptive confidence thresholding strategy. Therefore, further research should investigate alternative adaptive thresholding mechanisms, lightweight detection architectures, and their combinations to determine whether comparable robustness can be achieved with reduced computational and memory requirements. Future studies should also consider

larger and more diverse datasets containing greater variations in field conditions, illumination, background complexity, disease severity, and leaf scale.

REFERENCES:

1. Richter, D. J., Ilias Bappi, M., Sanjay Kolekar, S., and Kim, K. 2025. A Systematic Review of the Current State of Transfer Learning Accelerated CNN-Based Plant Leaf Disease Classification. IEEE Access. 116262–116303
2. Simhadri, C. G., Kondaveeti, H. K., Vatsavayi, V. K., Mitra, A., and Ananthachari, P. 2025. Deep learning for rice leaf disease detection: A systematic literature review on emerging trends, methodologies and techniques. Information Processing in Agriculture. 151–168
3. Harakannanavar, S. S., Rudagi, J. M., Puranikmath, V. I., Siddiqua, A., and Pramodhini, R. 2022. Plant leaf disease detection using computer vision and machine learning algorithms. Global Transitions Proceedings: 3(1): 305–310 doi: 10.1016/j.gltp.2022.03.016.
4. Shafik, W., Tufail, A., Namoun, A., De Silva, L. C., and Apong, R. A. A. H. M. 2023. A Systematic Literature Review on Plant Disease Detection: Motivations, Classification Techniques, Datasets, Challenges, and Future Trends. IEEE Access: 11: 59174–59203 doi: 10.1109/ACCESS.2023.3284760.
5. Narmadha, R. P. and Arulvadivu, G. 2017. Detection and measurement of paddy leaf disease symptoms using image processing. 2017 International Conference on Computer Communication and Informatics (ICCCI). 1–4
6. Prajapati, H. B., Shah, J. P., and Dabhi, V. K. 2017. Detection and classification of rice plant diseases. Intelligent Decision Technologies: 11(3): 357–373 doi: 10.3233/IDT-170301.
7. Dubey, R. K. and Choubey, D. K. 2025. Classification of Paddy Plant leaf diseases using optimized Support Vector Machine. Procedia Computer Science. 1619–1628
8. Amosedinakaran, S., Anitha, P., Kannan, R., Karthikeyan, K., Suresh, S., and Bhuvanesh, A. 2025. Paddy leaf disease identification and K-means cluster segmentation using multi-class SVM techniques. Measurement: Sensors: 42: doi: 10.1016/j.measen.2025.101979.
9. Wijayanto, A. K., Prasetyo, L. B., Hudjimartsu, S. A., Sigit, G., and Hongo, C. 2024. Textural features for BLB disease damage assessment in paddy fields using drone data and machine learning: Enhancing disease detection accuracy. Smart Agricultural Technology: 8: doi: 10.1016/j.atech.2024.100498.
10. Tasfe, M., Nivrito, A., Al MacHot, F., Ullah, M., and Ullah, H. 2024. Deep Learning Based Models for Paddy Disease Identification and Classification: A Systematic Survey. IEEE Access: 12: 100862–100891 doi: 10.1109/ACCESS.2024.3419708.
11. Matin, Md. M. H., Khatun, A., Moazzam, Md. G., and Uddin, M. S. 2020. An Efficient Disease Detection Technique of Rice Leaf Using AlexNet. Journal of Computer and Communications: 08(12): 49–57 doi: 10.4236/jcc.2020.812005.
12. Babu, S., Maravarman, M., and Pitchai, R. 2022. Detection of Rice Plant Disease Using Deep Learning Techniques. Journal of Mobile Multimedia: 18(3): 757–770 doi: 10.13052/jmm1550-4646.18314.
13. Petchiammal, A. and Murugan, D. 2025. Automated Paddy Leaf Disease Identification using Visual Leaf Images based on Nine Pre-trained Models Approach. Procedia Computer Science. 118–126

14. Padhi, J., Mishra, K., Ratha, A. K., Behera, S. K., Sethy, P. K., and Nanthaamornphong, A. 2025. Enhancing paddy leaf disease diagnosis -a hybrid CNN model using simulated thermal imaging. Smart Agricultural Technology: 10: doi: 10.1016/j.atech.2025.100814.
15. Mehnaz, S. and Islam, Md. T. 2025. Rice Leaf Disease Detection: A Comparative Study Between CNN, Transformer and Non-neural Network Architectures
16. Ramesh, S. and Vydeki, D. 2020. Recognition and classification of paddy leaf diseases using Optimized Deep Neural network with Jaya algorithm. Information Processing in Agriculture: 7(2): 249–260 doi: 10.1016/j.inpa.2019.09.002.
17. Singh, J. P., Ghosh, D., Kumar, A., Bilgaiyan, S., Kumar, R., and Singh, J. 2026. Hybrid DenseNet Architectures and KerasTuner-Based Optimization for Rice Leaf Disease Detection. IEEE Access: 14: 26845–26868 doi: 10.1109/ACCESS.2026.3664467.
18. Tasci, M. 2026. DBLA-MobileNetV2: Real-Time Rice Leaf Disease Detection on Edge Devices With Dual-Branch Lightweight Attention. IEEE Access: 14: 22356–22371 doi: 10.1109/ACCESS.2026.3662799.
19. Altabaji, W. I. A. E., Umair, M., Tan, W. H., Foo, Y. L., and Ooi, C. P. 2024. Comparative Analysis of Transfer Learning, LeafNet, and Modified LeafNet Models for Accurate Rice Leaf Diseases Classification. IEEE Access: 12: 36622–36635 doi: 10.1109/ACCESS.2024.3373000.
20. Mahadevan, K., Punitha, A., and Suresh, J. 2024. A novel rice plant leaf diseases detection using deep spectral generative adversarial neural network. International Journal of Cognitive Computing in Engineering: 5: 237–249 doi: 10.1016/j.ijcce.2024.05.004.
21. Joseph, D. S., Pawar, P. M., and Chakradeo, K. 2024. Real-Time Plant Disease Dataset Development and Detection of Plant Disease Using Deep Learning. IEEE Access: 12: 16310–16333 doi: 10.1109/ACCESS.2024.3358333.
22. Bijoy, M. H., Hasan, N., Biswas, M., Mazumdar, S., Jimenez, A., Ahmed, F., Rasheduzzaman, M., and Momen, S. 2024. Towards Sustainable Agriculture: A Novel Approach for Rice Leaf Disease Detection Using dCNN and Enhanced Dataset. IEEE Access: 12: 34174–34191 doi: 10.1109/ACCESS.2024.3371511.
23. Uriel Rodrigo, K. K., Hillary Heart Marcial, J. S., Brillo, S. C., Mata, K. E., Morano, J. C., and Author, C. 2024. An Enhancement of CNN Algorithm for Rice Leaf Disease Image Classification in Mobile Applications. Journal of Information Systems Engineering and Management
24. Mahmud, T., Akter, M. S., Akter, T., Shahadat Hossain, M., and Andersson, K. 2025. Exploring Deep Learning and Explainable AI for Precise Rice Leaf Disease Detection and Classification. IEEE Access: 13: 162821–162844 doi: 10.1109/ACCESS.2025.3609671.
25. Jain, S., Sahni, R., Khargonkar, T., Gupta, H., Verma, O. P., Sharma, T. K., Bhardwaj, T., Agarwal, S., and Kim, H. 2022. Automatic Rice Disease Detection and Assistance Framework Using Deep Learning and a Chatbot. Electronics (Switzerland): 11(14): doi: 10.3390/electronics11142110.
26. Shahriar Zaman Abid, M., Jahan, B., Mamun, A. Al, Jakir Hossen, M., and Hossain Mazumder, S. 2024. Bangladeshi crops leaf disease detection using YOLOv8. Heliyon: 10(18): doi: 10.1016/j.heliyon.2024.e36694.

27. Tripathi, A., Gohokar, V., and Kute, R. 2024. Comparative Analysis of YOLOv8 and YOLOv9 Models for Real-Time Plant Disease Detection in Hydroponics. Engineering, Technology and Applied Science Research: 14(5): 17269–17275 doi: 10.48084/etasr.8301.
28. Sudharshan, B. S., Avinaas, S. V. D., Sujith, U., and Anitha, G. 2025. Rice Leaf Disease Detection using YOLOv9.
29. Zope, S., Patil, M., Lakshmi, Bs., Borase, S., Jayprakash Patel, P., Waghmare, G. H., and Vadivukarasi, L. 2024. Nanotechnology Perceptions ISSN 1660-6795 www. Nanotechnology Perceptions
30. Wang, C.-Y., Yeh, I.-H., and Liao, H.-Y. M. 2024. YOLOv9: Learning What You Want to Learn Using Programmable Gradient Information
31. He, K., Zhang, X., Ren, S., and Sun, J. 2016. Deep Residual Learning for Image Recognition. 2016 IEEE Conference on Computer Vision and Pattern Recognition (CVPR). 770–778
32. Ren, S., He, K., Girshick, R., and Sun, J. 2016. Faster R-CNN: Towards Real-Time Object Detection with Region Proposal Networks
33. Hasan, M. 2023. Rice Leaf Bacterial and Fungal Disease Dataset. Mendeley Data